

FINAL
12-13-CR
4 REC
6073
p. 21

FINAL TECHNICAL REPORT
NASA Cooperative Agreement NCC-1-151

SHIELDING MATERIALS
FOR HIGHLY PENETRATING SPACE RADIATIONS

November 14, 1995

Principal Investigators: RICHARD L. KIEFER
ROBERT A. ORWOLL

Grantee Institution: THE COLLEGE OF WILLIAM AND MARY
WILLIAMSBURG, VIRGINIA 23187

(NASA-CR-199720) SHIELDING
MATERIALS FOR HIGHLY PENETRATING
SPACE RADIATIONS Final Report
(College of William and Mary) 21 p

N96-14600

Unclass

G3/18 0077061

SHIELDING MATERIALS FOR HIGHLY PENETRATING SPACE RADIATIONS

Introduction

Interplanetary travel involves the transfer from an Earth orbit to a solar orbit. Once outside the Earth's magnetosphere, the major sources of particulate radiation are solar cosmic rays (SCRs) and galactic cosmic rays (GCRs). Intense fluxes of SCRs come from solar flares and consist primarily of protons with energies up to 1 GeV. The GCR consists of a low flux of nuclei with energies up to 10^{10} GeV. About 70% of the GCR are protons, but a small amount (0.6%) are nuclei with atomic numbers greater than 10.¹ High energy charged particles (HZE) interact with matter by transferring energy to atomic electrons in a Coulomb process and by reacting with an atomic nucleus. Energy transferred in the first process increases with the square of the atomic number, so particles with high atomic numbers would be expected to lose large amounts of energy by this process. Nuclear reactions produced by (HZE) particles produce high-energy secondary particles which in turn lose energy to the material. The HZE nuclei are a major concern for radiation protection of humans during interplanetary missions because of the very high specific ionization of both primary and secondary particles.²

Computer codes have been developed to calculate the deposition of energy by very energetic charged particles in various materials³. Calculations show that there is a significant buildup of secondary particles from nuclear fragmentation and Coulomb dissociation processes. A large portion of these particles are neutrons.

Since neutrons carry no charge, they only lose energy by collision or reaction with a nucleus. Neutrons with high energies transfer large amounts of energy by inelastic collisions with nuclei. However, as the neutron energy decreases, elastic collisions become much more effective for energy loss. The lighter the nucleus, the greater the fraction of the neutron's kinetic energy that can be lost in an elastic collision. Thus, hydrogen-containing materials such as polymers are most effective in reducing the energy of neutrons.

Once neutrons are reduced to very low energies, the probability for undergoing a reaction with a nucleus (the cross section) becomes very high. The product of such a reaction is often radioactive and can involve the release of a significant amount of energy. Thus, it is important to provide protection from low energy neutrons during a long duration space flight.

Among the light elements, lithium and boron each have an isotope with a large thermal neutron capture cross section, ^6Li and ^{10}B . However, as shown in Figure 1,

^{10}B is more abundant in the naturally-occurring element than ^6Li , has a thermal neutron capture cross section four times that of ^6Li , and produces the stable products, ^4He and ^7Li in the interaction while ^6Li produces radioactive tritium (^3H). Thus, boron is the best light-weight material for thermal neutron absorption in spacecraft.

The work on this project was focused in two areas: computer design where existing computer codes were used, and in some cases modified, to calculate the propagation and interactions of high energy charged particles through various media, and materials development where boron was incorporated into high performance materials.

Computer Design

Calculations were performed by a graduate student, Myung-Hee Kim, in collaboration with members of the Environmental Interactions Branch of the Materials Division, particularly Dr. John Wilson. An energy-dependent high energy heavy-ion transport code, modified by Wilson *et al.*⁴, was used. The code is a modification of LBLFRG, a model based on Boltzmann transport theory. The fluence of particles emitted from the back of a target irradiated with a high-energy heavy-ion beam was calculated. Collisions of the primary particle will create projectile fragments with a charge less than that of the original particle, and target fragments. Projectile fragments usually continue on with very nearly the velocity of the primary ion. Having sufficiently high energy, the projectile fragments may collide with atomic nuclei in thick shields and create a second generation of fragments, and so on. Target fragments are emitted from a struck target nucleus usually with a much lower energy than projectile fragments and isotropically in the rest frame of the target.

The computer code was used to predict the fragment fluence for a beam of ^{56}Fe ions at an energy of about 600 MeV/amu incident on a variety of targets: an epoxy, lunar regolith, regolith with epoxy, polyethylene, polytetrafluoroethylene, a polysulfone, a polyimide, a polyetherimide and the polyetherimide containing of boron powder. The epoxy chosen was tetraglycidyl 4,4'-diamino diphenyl methane (TG 4,4'DDM) cured with diamino diphenyl sulfone (DDS). The chemical structure of the cured material is shown in Figure 2. Figure 3 shows the structures of the polyetherimide, the polysulfone, and the polyimide. The attenuation of a beam of ^{56}Fe ions with an energy of 605 MeV/amu through various targets is shown in Figures 4, 5, and 6. The energy of the ^{56}Fe beam was chosen to coincide with an experiment run at the BEVALAC accelerator in California. The data from that experiment have not yet been analyzed. In all materials, the target thickness exceeds the range of the incident ^{56}Fe beam in that material, so no iron particles ($Z = 26$) are emitted at the back of the target. For each figure, it can be seen that the greatest attenuation comes from the material which contains the largest mass percent of

hydrogen. This occurs because hydrogen has the greatest cross section per unit mass for these interactions.⁵ There is only a small difference between the fluence behind a shield of the pure polyetherimide and that of the polymer containing boron indicating that the addition of boron to a hydrogen-containing polymer does not significantly change its effectiveness as a cosmic ray shield. The difference reflects the fact that the boron-containing materials have a slightly lower percentage of hydrogen.

The effectiveness of materials for biological shielding was examined in terms of two models. The first was the conventional risk assessment method using the quality factor as a function of linear energy transfer (LET). The dose equivalent for radiation penetrating a shield of thickness, x , is designated $H(x)$. It was obtained by multiplying the absorbed dose at each LET value by a corresponding quality factor⁶, and is a measure of the response of living tissue to absorbed radiation. The relative attenuation of dose equivalent, $H(x)/H(0)$, as a function of shield thickness is shown in Figures 7 and 8, where $H(0)$ is the dose equivalent in free space, i.e., with no shield.

The second model is a track-structure repair model for the mouse cell C3H10T1/2.⁷ This is the response of living cells to GCRs in terms of occurrences of neoplastic cell transformations, $T(x)$, resulting from a one-year exposure behind a shield of thickness, x , relative to occurrences, $T(0)$, in free space. This model differs from the previous one in that it is driven by track-structure-dependent injury coefficients from experimental data with various ion beams in the mouse cell C3H10T1/2. The variation in the calculated cell transformation ratio, $T(x)/T(0)$, is shown in Figures 9 and 10. It appears that the dependence on material is qualitatively similar for $H(x)/H(0)$ and $T(x)/T(0)$. However, there are important quantitative differences. For example, a 20 g/cm² shield of lunar regolith has a dose equivalent ratio, $H(x)/H(0)$, of about 0.5, but a cell transformation ratio, $T(x)/T(0)$, of about 0.75. Such a difference could be critical for long-term space exposures. Shield optimization must await an improved understanding of biological responses.

Materials Development

Shielding which combines a hydrogen-containing polymeric material with boron would be desirable to shield humans from neutron irradiation. In space, the polymer would be exposed to radiation over an extended period of time. Thus, it is important to choose materials which are known to have good stability toward radiation. For this reason, we incorporated boron into the four polymeric materials shown in Figures 1 and 2, all of which are known to have good stability toward radiation.

Films of the polyimide, polypyromellitimide, were made by drawing the

corresponding polyamic acid over a glass plate and heating to 300°C. The resulting material is extremely stable toward degradation from charged particle radiation.⁸ Films containing boron were made by mixing submicron boron powder with the polyamic acid before the mixture was drawn across the glass plate. The polyetherimide was dissolved in chloroform and the solution was drawn over a glass plate. The solvent is slowly evaporated producing a good film. The effects of energetic electrons on this material have been well studied.⁹ Submicron boron powder was added to the polymer solution and mixed thoroughly before the solution was drawn across the glass plate to produce films containing up to 20% boron by mass. Films of the polysulfone were made in the same manner as those of the polyetherimide. The effects of ionizing radiation on this material has also been well documented.¹⁰

The epoxy selected was ICI Fiberite's 934, which is an aerospace-qualified resin. Initially, the uncured epoxy resin and the boron were thoroughly mixed at 66 to 71° C where the viscosity of the resin was low enough for mixing to occur. The mixture was then poured into a mold and cured by increasing the temperature 1 to 3° C per minute up to 121° C, holding the temperature there for one hour, then increasing the temperature at the same rate up to 177° C and holding it there for two hours. A scanning electron micrograph showed that the distribution of the boron powder was not uniform. A second method of mixing was tried in which the resin and boron powder were mixed at a temperature of about -30° C in a walk-in freezer. The solid resin and boron powder were ground together in a large mortar, followed by transfer of the mixed powder to the mold and curing with the same temperature profile as before. The results appeared to be somewhat better, but still not totally satisfactory. Not surprisingly, the distribution of boron in the films was much better. Figure 11 is a scanning electron micrograph of a polyetherimide film containing 20 percent by mass of boron. The white dots are the submicron particles of boron. As the micrograph shows, the boron is uniformly distributed throughout the film.

The boron loaded polyetherimide films have been tested for their ability to absorb thermal neutrons. A disk of 4 mil indium foil approximately 3 cm in diameter was wrapped with films containing boron and irradiated with thermal neutrons in a 5 curie plutonium/beryllium neutron source. A radioactive isotope of indium, ¹¹⁶In, is formed by the thermal neutron capture of ¹¹⁵In (95.7% of natural indium). The film-wrapped indium disk was irradiated for approximately 12 hours, long enough to saturate the production of the ¹¹⁶In which has a half life of 54.1 minutes. The radioactive indium was counted for about two half lives and the initial activity (the activity when the foil was removed from the neutron source) was determined. When the indium was wrapped with a polyetherimide film containing no boron, the initial activity was about 13,000 counts per minute. When a film containing 20 percent boron by mass surrounded the indium, the initial activity was about 9,700 counts per minute. Figures 12 and 13 show the counting data for these two exposures plotted as a function of time. Films containing 5, 10 and 15 percent boron by mass were also

tested in the same manner. Figure 14 shows the initial activity of the indium foil as a function of the percent boron in the film surrounding it. In each a 4 mil thickness of the polymer film was used.

Chemical analyses of the boron-containing materials by inductively-coupled plasma (ICP) revealed that the actual percentage of boron was generally lower than calculated. This is probably due to incomplete mixing and the tendency of the boron powder to creep up the sides of the container in the polymer solutions.

Conclusions

A theoretical study was initiated to investigate the interaction and alteration of space radiations by various materials in order to select ones that will most significantly reduce the risk to humans from exposure to the high energy heavy ion component of galactic cosmic rays.

The effects of hydrogen-containing materials as potential space structural components were examined by comparing the total ion fluence after passing through a given thickness of the material. For energetic ion beams of ^{56}Fe , a polyethylene shield with its high hydrogen density is the most effective absorber when the material is thick enough to stop the incident beam particles. Adding an epoxy to lunar regolith enhances its shielding characteristics. The inclusion of boron in a polymeric material only slightly diminishes the capacity of the material to absorb the high energy heavy ions.

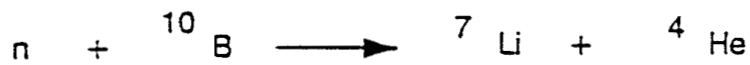
Biological effects from radiation depend on the microscopic fluctuations of energy absorption events in specific tissues.¹¹ These effects are reduced not only by selecting appropriate materials, but also by adjusting the thickness of the material. Because of its high hydrogen density, polyethylene is an efficient shield material for GCRs at all thicknesses. There are important quantitative differences between the two biological models used in these studies.

One result of the interaction of GCRs with materials is the production of neutrons. The energy of neutrons is most effectively reduced by elastic collisions with hydrogen (protons). Polymeric materials containing hydrogen are thus both effective in absorbing GCRs and effective in reducing the energy of neutrons. Once neutrons are reduced in energy, they are very efficiently absorbed by an isotope of boron, ^{10}B . Submicron boron powder has been incorporated into several high performance polymers and into an aerospace-qualified epoxy resin. In thin polymer films, the boron powder appears to be uniformly distributed, but in thick epoxy samples, the boron appears to form clusters. Polymeric materials containing up to 20% by mass of boron are effective absorbers of low-energy neutron.

References

1. G. R. Choppin and J. Rydberg, *Nuclear Chemistry - Theory and Applications*, Pergamon Press, New York (1980) p. 78.
2. J. W. Wilson, L. W. Townsend, W. Schimmerling, G. S. Khandelwal, F. Khan, J. E. Nealy, F. A. Cucinotta, L. C. Simonsen, J. L. Shinn, and J. W. Norbury, "Transport Methods and Interactions for Space Radiations," *NASA RP-1257*, Washington D.C., 1994.
3. L. W. Townsend, J. E. Nealy, J. W. Wilson, and L. C. Simonsen, "Estimates of Galactic Cosmic Ray Shielding Requirements During Solar Minimum," *NASA TM-4167*, 1990.
4. J. W. Wilson, S. L. Lamkin, H. Farhat, B. D. Ganapol, and L. W. Townsend, "A Hierarchy of Transport Approximations for High Energy Heavy (HZE) Ions," *NASA TM-4118*, 1989.
5. M. Y. Kim, J. W. Wilson, S. A. Thibeault, J. E. Nealy, F. F. Badavi, and R. L. Kiefer, "Performance Study of Galactic Cosmic Ray Shield Materials," *NASA TP-3473*, 1994.
6. International Commission on Radiological Protection, *1990 Recommendations of the International Commission on Radiological Protection*, ICRP Publ. 60, p 81, Pergamon, New York (1991).
7. J. W. Wilson, F. A. Cucinotta, and J. L. Shinn, "Cell Kinetics and Track Structure," in *Biological Effects and Physics of Solar and Galactic Cosmic Radiation, Part B*, C. E. Swenberg, G. Horneck, and E. G. Stassinopoulos, eds., Plenum Press, New York, pp 295-338, 1993.
8. D. R. Coulter, A. Gupta, M. V. Smith, and R. E. Fornes, "The Effects of Energetic Proton Bombardment on Polymeric Materials: Experimental Studies and Degradation Models," *NASA JPL Publication 85-101*, 1986.
9. S. A. T. Long and E. R. Long, Jr., "Effects of Intermediate-Energy Electrons on Mechanical and Molecular Properties of a Polyetherimide," *IEEE Trans. Nucl. Sci.*, **NS-31**, 1293 (1984).
10. J. R. Brown and J. H. O'Donnell, "Effects of Gamma Radiation on Two Aromatic Polysulfones," *J. Appl. Poly. Sci.*, **19**, 405 (1975).
11. J. W. Wilson, M. Y. Kim, W. Schimmerling, F. F. Badavi, S. A. Thibeault, F. A. Cucinotta, J. L. Shinn, and R. L. Kiefer, "Issues in Space Radiation Protection: Galactic Cosmic Rays," *Health Physics*, **68**, pp 50-58 (1995).

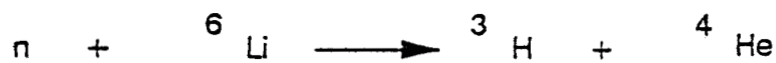
USE OF BORON VS. LITHIUM



19.8% of
natural B

stable products

relative reaction probability = 1.0



7.5% of
natural Li

radioactive product

relative reaction probability = 0.25

Figure 1. A comparison of boron and lithium as absorbers of thermal neutrons.

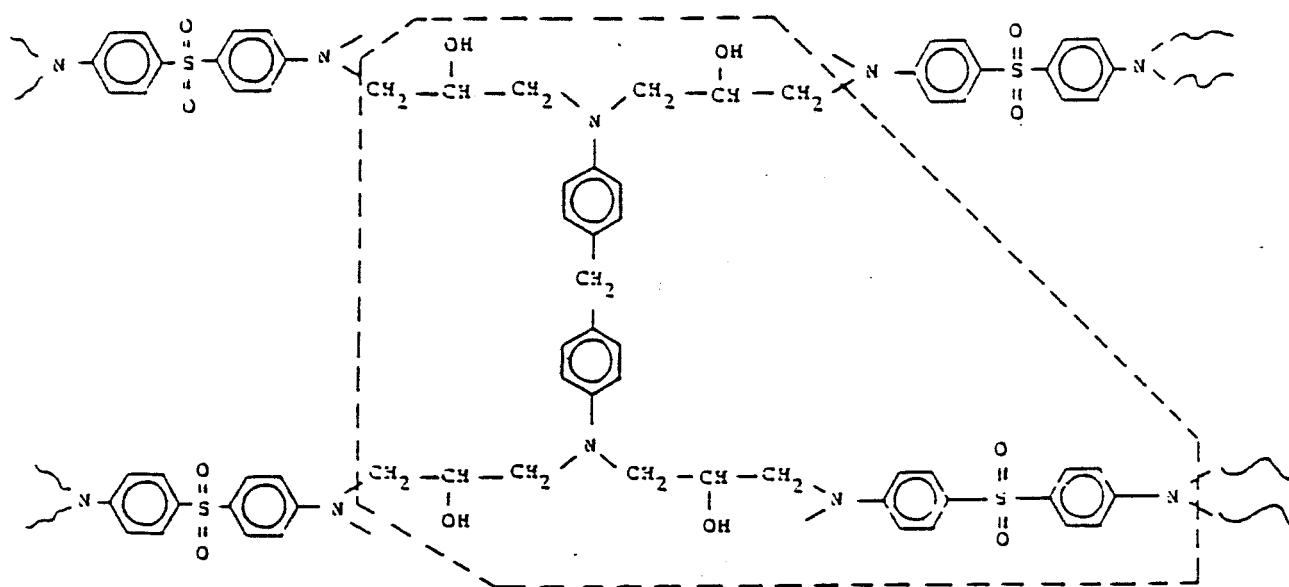
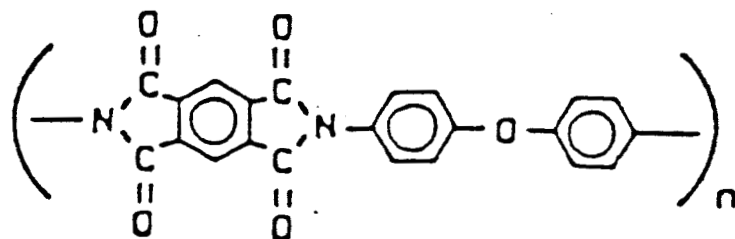
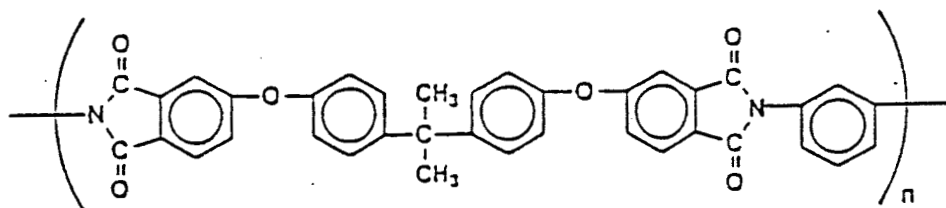


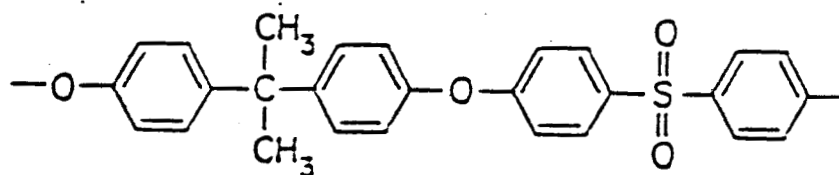
Figure 2. The repeat unit of tetraglycidyl 4,4'-diamino diphenyl methane epoxy cured with diamino diphenyl sulfone.



The repeat unit of the polyimide, polypyromellitimide.



The repeat unit of the polyeherimide.



The repeat unit of the polysulfone.

Figure 3. The repeat units of three polymeric materials studied.

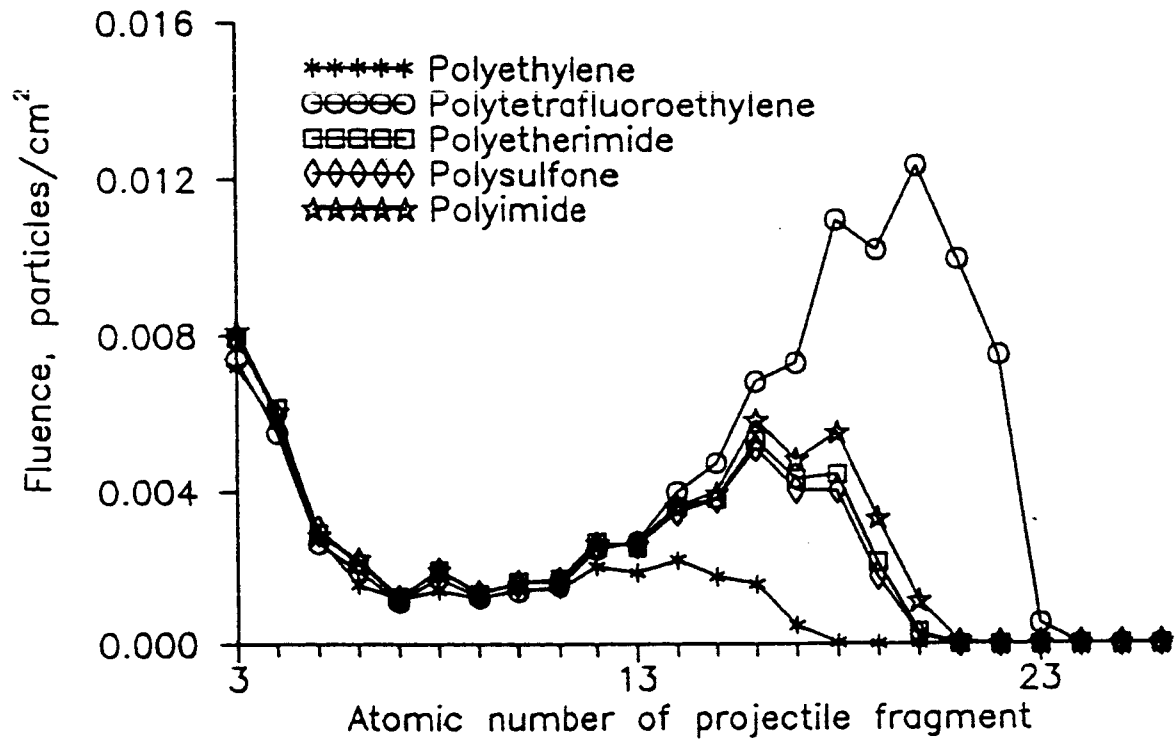


Figure 4. The calculated fluence of projectile fragments behind 18 g/cm³ thick polymeric shields with 605 MeV/amu (33.88 GeV) ⁵⁶Fe ions.

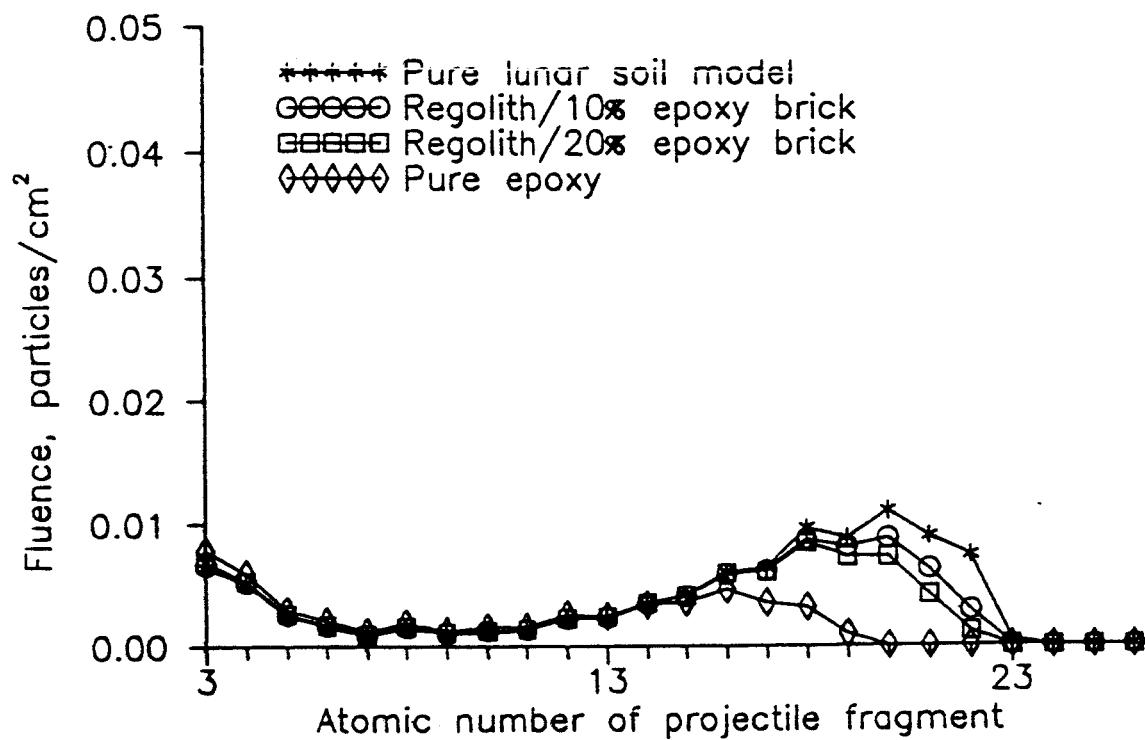


Figure 5. The calculated fluence of projectile fragments behind 18 g/cm³ thick lunar construction materials with 605 MeV/amu (33.88 GeV) ⁵⁶Fe ions.

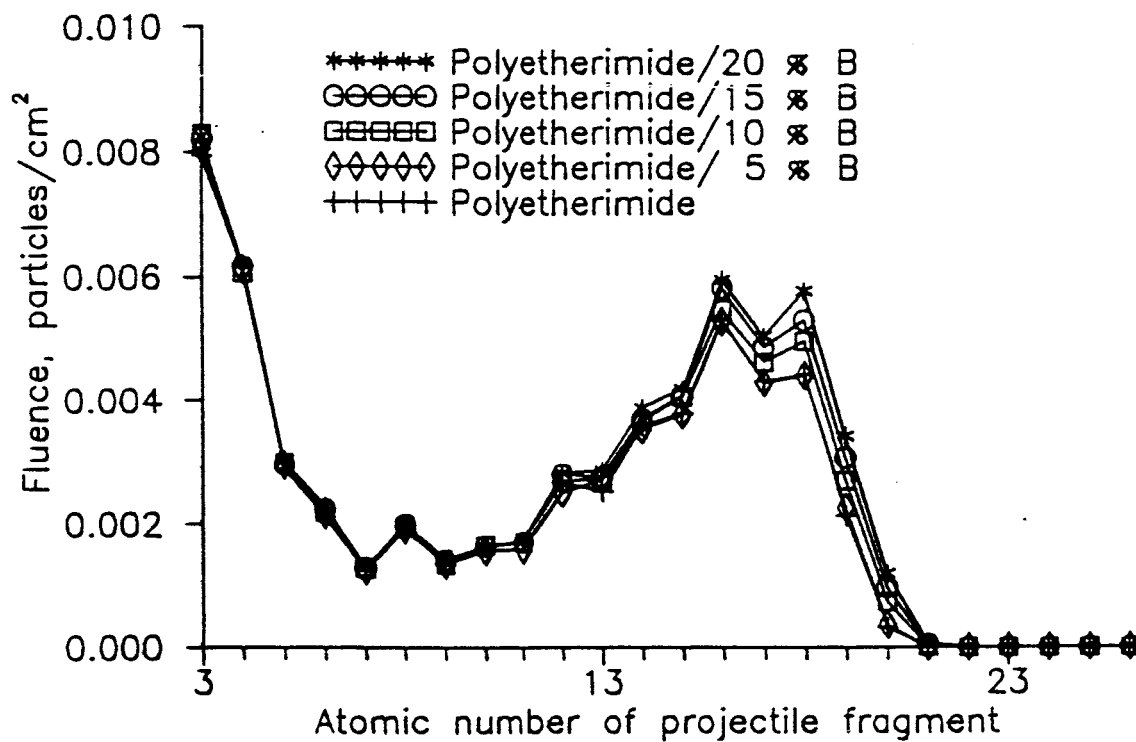


Figure 6. The calculated fluence of projectile fragments behind 18 g/cm³ thick polyetherimide shields containing differing weight fractions of boron with 605 MeV/amu (33.88 GeV) ⁵⁶Fe ions.

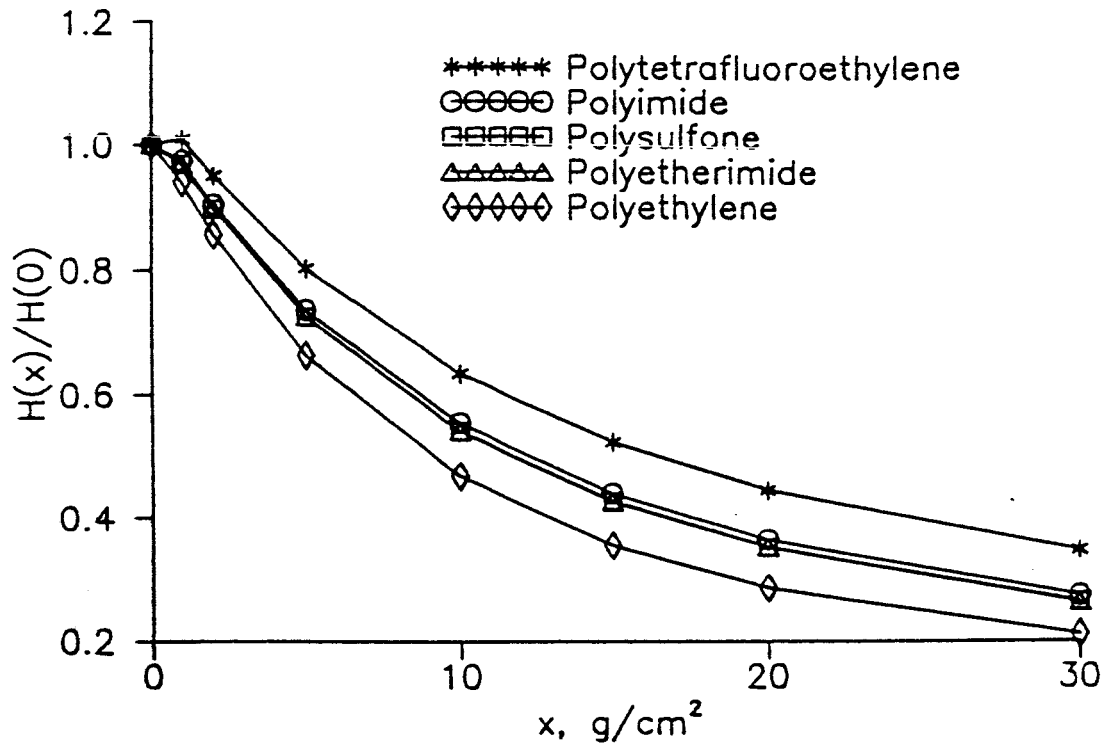


Figure 7. Attenuation of dose equivalent in a one-year GCR exposure behind polymeric shields as a function of shield thickness.

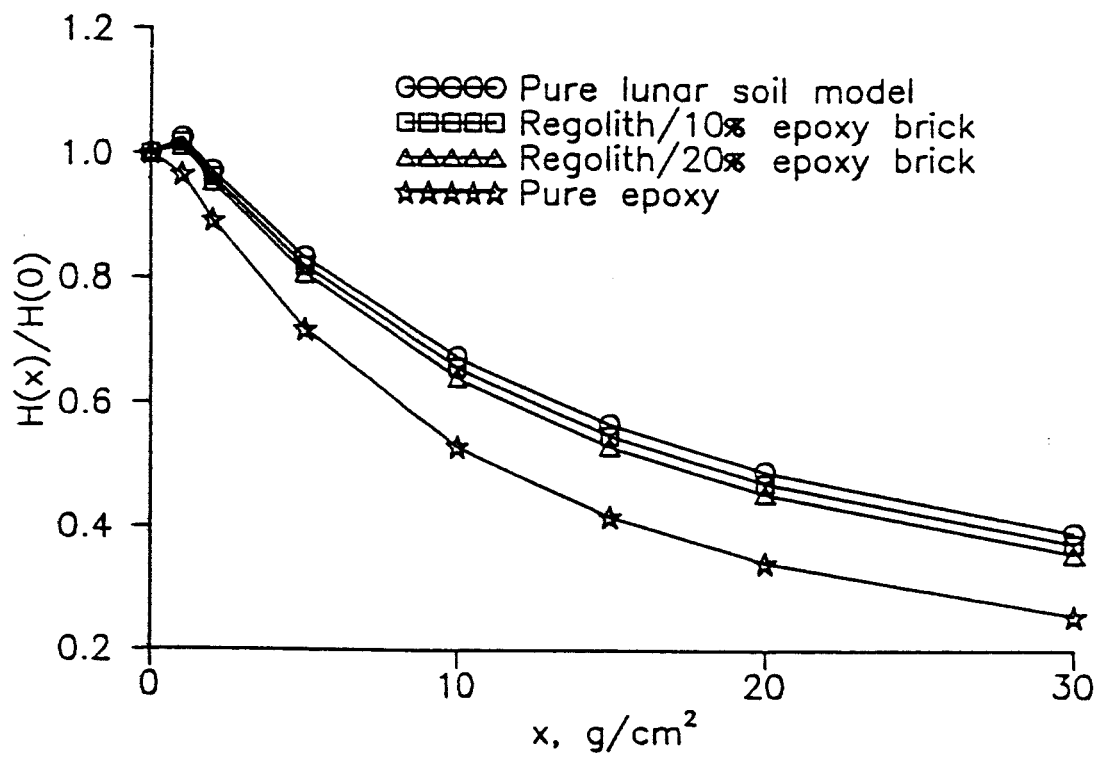


Figure 8. Attenuation of dose equivalent in a one-year GCR exposure behind lunar construction materials as a function of shield thickness.

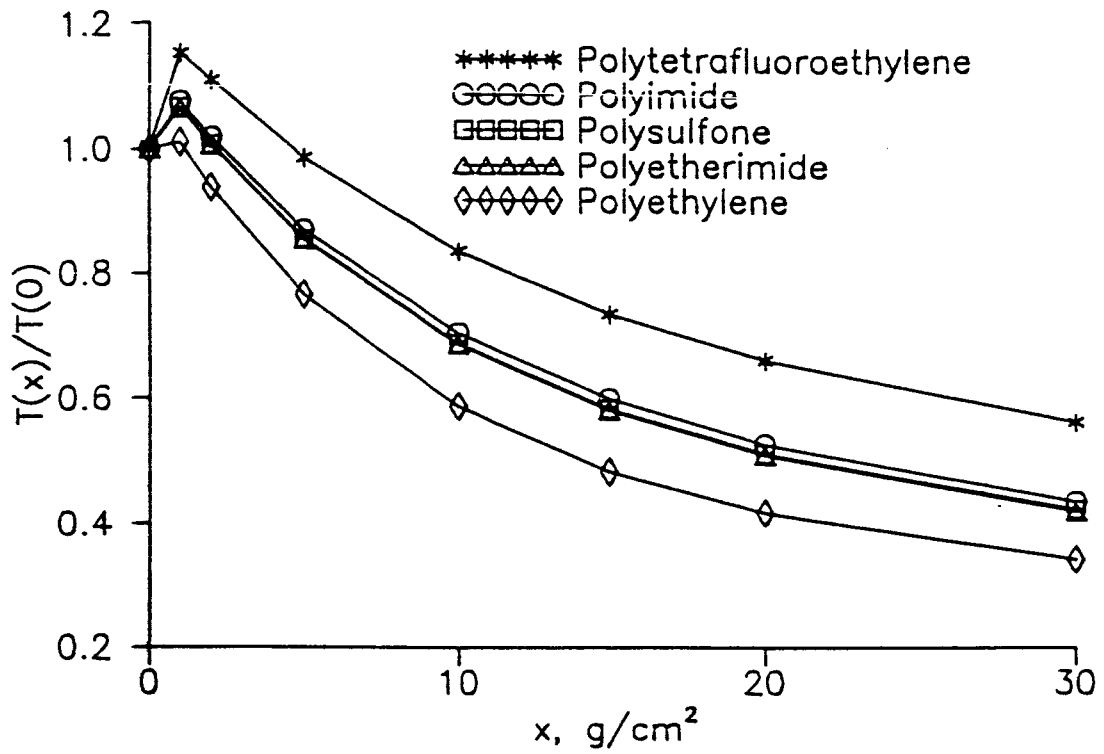


Figure 9. Attenuation of cell transformation in a one-year GCR exposure behind polymeric shields as a function of shield thickness.

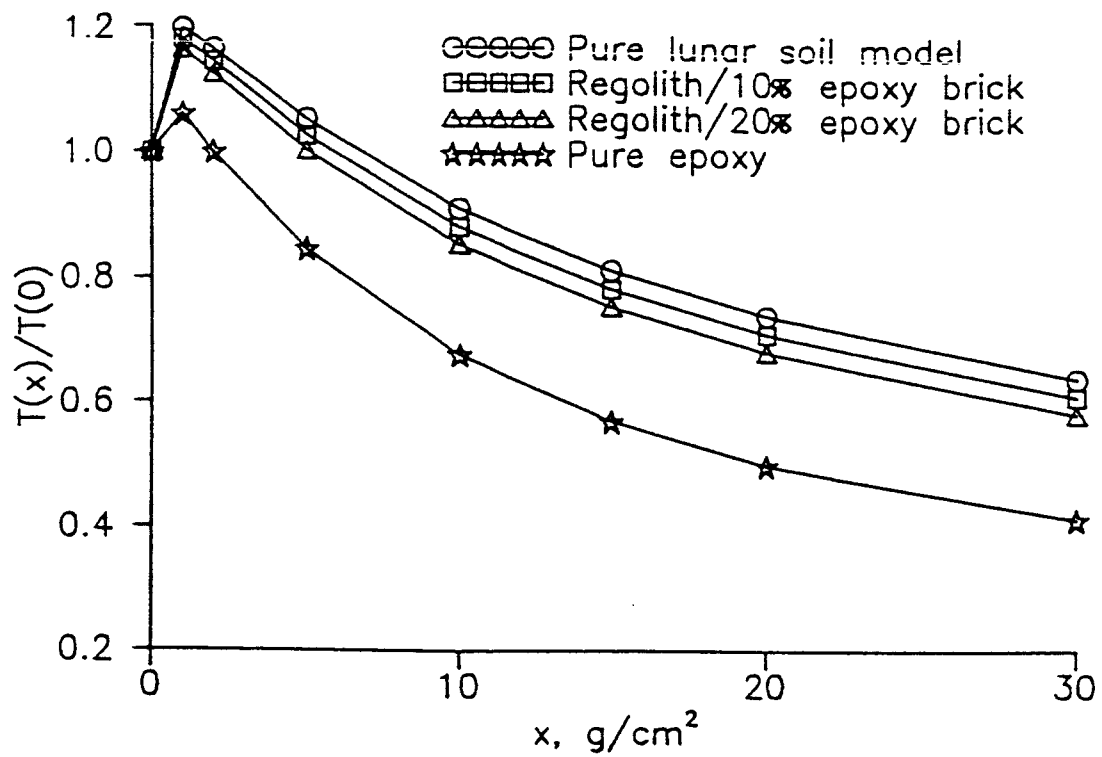


Figure 10. Attenuation of cell transformation in a one-year GCR exposure behind lunar construction materials as a function of shield thickness.

SCANNING ELECTRON MICROGRAPH
POLYETHERIMIDE WITH 20% BORON POWDER

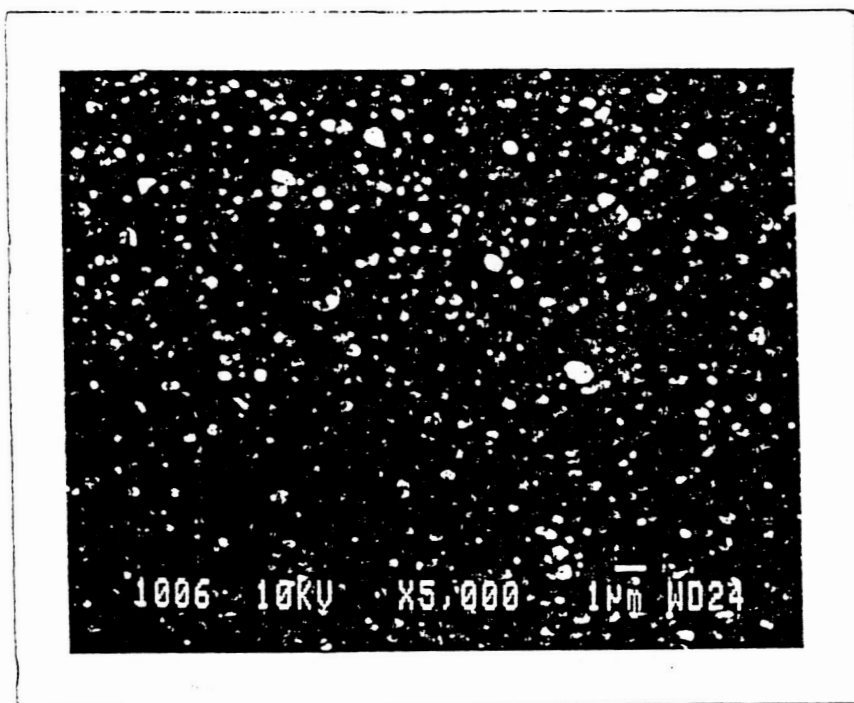


Figure 11. A scanning electron micrograph of a film of polyetherimide containing 20% by mass of submicron boron powder.

ACTIVITY OF INDIUM FOIL SURROUNDED BY
4 MILS OF FILM CONTAINING 0% BORON

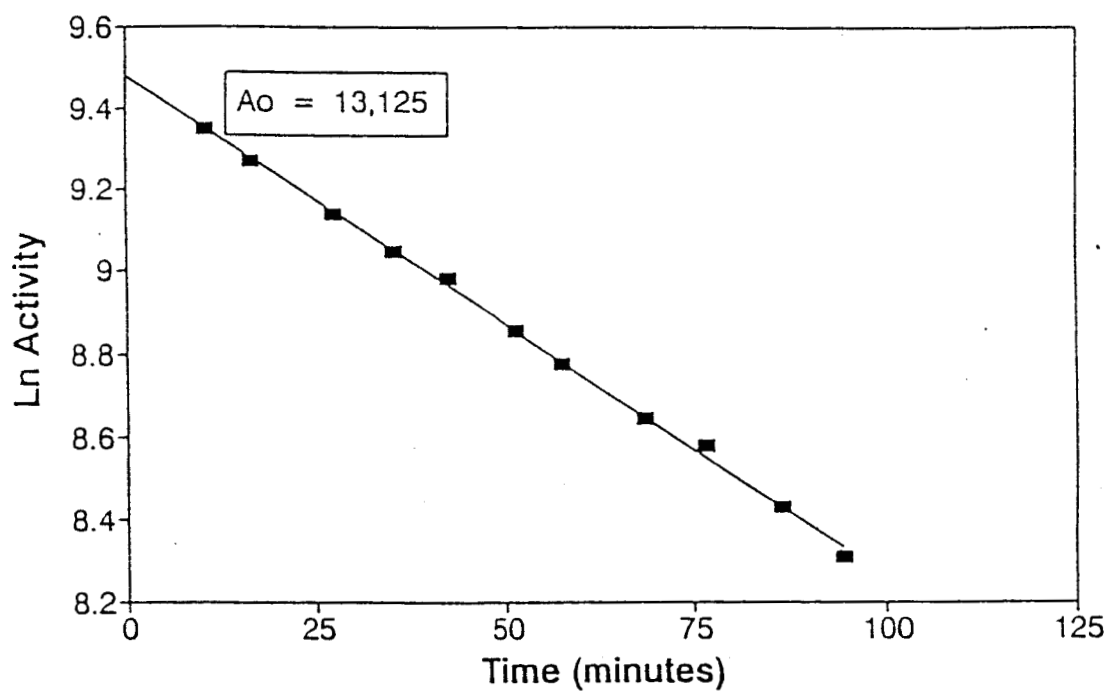


Figure 12. The decay of an activated indium foil surrounded by 4 mils of pure polyetherimide film.

ACTIVITY OF INDIUM FOIL SURROUNDED BY
4 MILS OF FILM CONTAINING 20% BORON

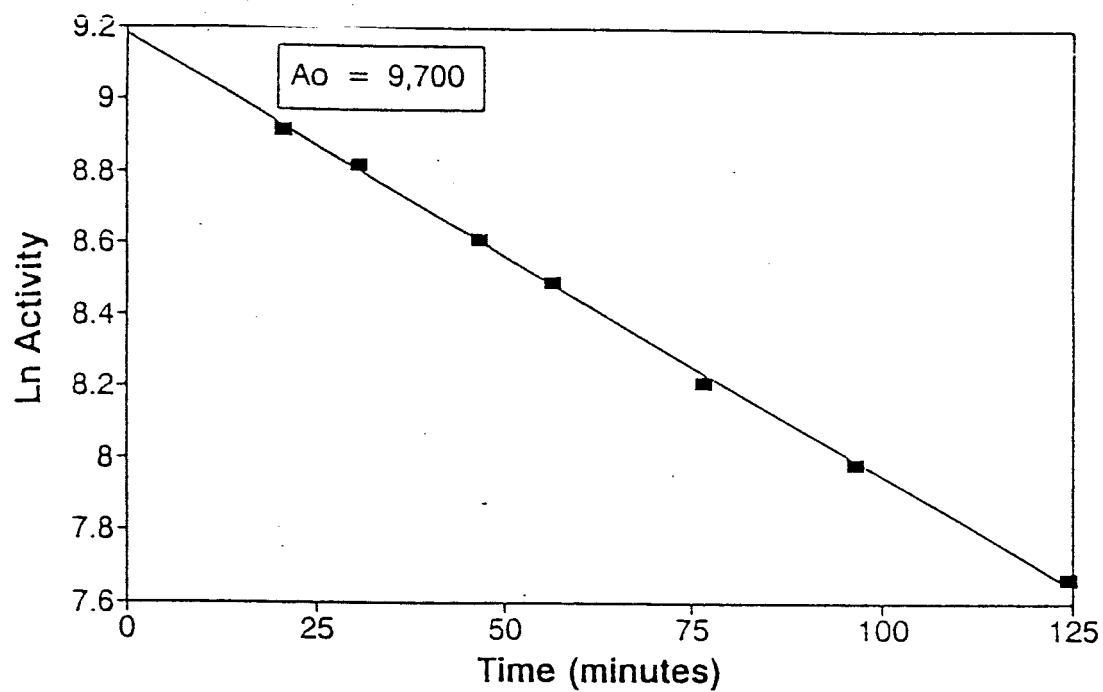


Figure 13. The decay of an activated indium foil surrounded by 4 mils of polyetherimide film containing 20% boron.

EFFECTS OF WEIGHT % BORON IN FILMS

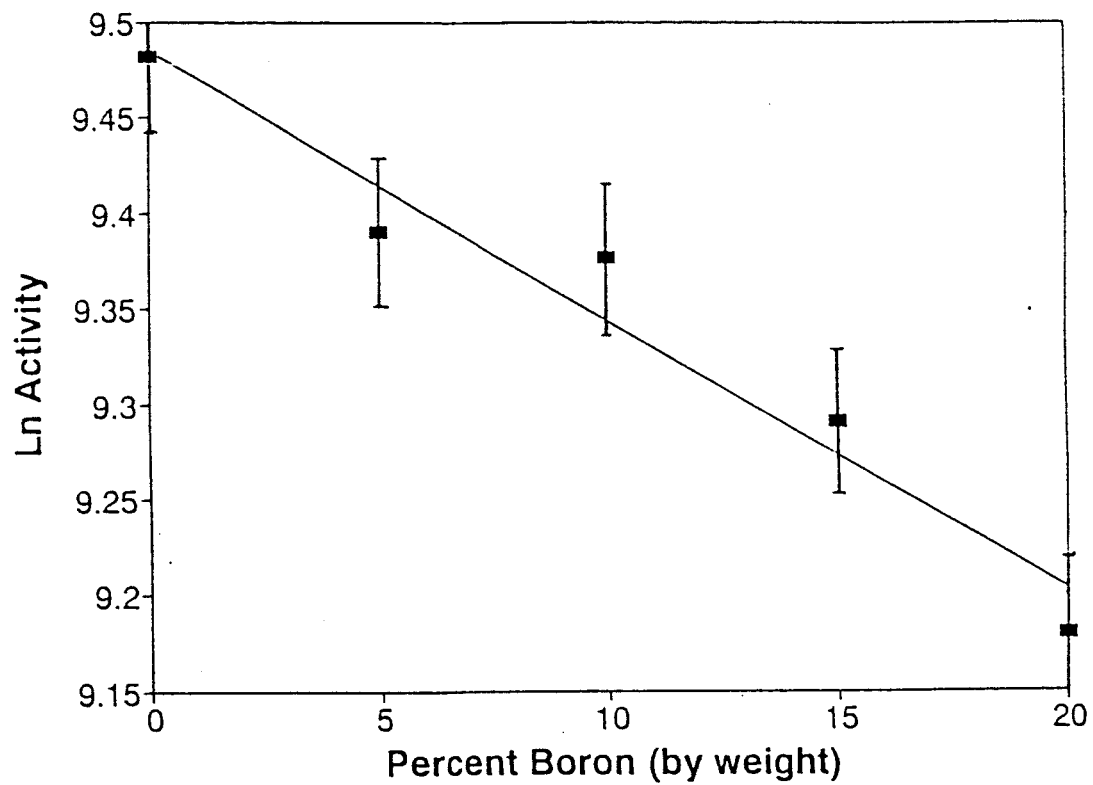


Figure 14. The initial activity of an indium foil as a function of the percent boron in the film surrounding it during activation.